Molecular Crystals and Liquid Crystals

ISSN: 1542-1406 (Print) 1563-5287 (Online) Journal homepage: http://www.tandfonline.com/loi/gmcl20

Efficiency Enhancement of Polymer Solar Cells with Three-Component Active Layer

Seonju Jeong & Yoon Soo Han

To cite this article: Seonju Jeong & Yoon Soo Han (2015) Efficiency Enhancement of Polymer Solar Cells with Three-Component Active Layer, Molecular Crystals and Liquid Crystals, 620:1, 53-63, DOI: 10.1080/15421406.2015.1094863

To link to this article: http://dx.doi.org/10.1080/15421406.2015.1094863

Published online: 16 Dec 2015.

Submit your article to this journal

Article views: 8

View related articles

View Crossmark data

Full Terms & Conditions of access and use can be found at
http://www.tandfonline.com/action/journalInformation?journalCode=gmcl20

Download by: [East China University of Science and Technology] **Date:** 02 January 2016, At: 09:35

Mol. Cryst. Liq. Cryst., Vol. 620: pp. 53–63, 2015
Copyright © Taylor & Francis Group, LLC
ISSN: 1542-1406 print/1563-5287 online
DOI: 10.1080/15421406.2015.1094863

Downloaded by [East China University of Science and Technology] at 09:35 02 January 2016

Efficiency Enhancement of Polymer Solar Cells with Three-Component Active Layer

SEONJU JEONG[1] AND YOON SOO HAN[2,*]

[1]Graduate School of Energy, Environment, Water, and Sustainability (EEWS), Korea Advanced Institute of Science and Technology (KAIST), Daejeon, Korea
[2]Department of Advanced Materials and Chemical Engineering, Catholic University of Daegu, Gyeongbuk, Korea

*The photvoltaic performance of polymer solar cell (PSC) with a three-component active layer was studied. The incorporation of 4-cyano-4'-octylbiphenyl (*8CB*) as an additive to a P3HT [poly(3-hexylthiophene)]:$PC_{61}BM$ [[6,6]-phenyl-C61-butyric acid methyl ester] blend film led to a higher absorbance, larger crystal size, closer packing of P3HT, and hence enhanced hole mobility. The power conversion efficiency of the PSC with the three-component active layer (P3HT: $PC_{61}BM$:*8CB *blend film) was improved by over 30% compared to that of the reference device without* 8CB*, due to an enhancement in all parameters such as short circuit current, open circuit voltage and fill factor.*

Keywords polymer solar cell; 4-cyano-4'-octylbiphenyl; additive; P3HT; $PC_{61}BM$

Introduction

The current status of photovoltaics is that it hardly contributes to the energy market, because it is far too expensive. The large production costs for the silicon solar cells is one of the major obstacles. From this perspective, polymer solar cells (PSCs) based on blends of conjugated polymers and soluble fullerene derivatives are a promising and new renewable resource for the generation of electrical energy primarily due to their low manufacturing costs [1–3]. However, the power conversion efficiency (PCE) of PSCs is not sufficient for the realistic specifications necessary for commercial use. A bulk hetero-junction (BHJ) structure [4–6] composed of poly(3-hexylthiophene) (P3HT, electron donor) and [6,6]-phenyl-C_{61}-butyric acid methyl ester ($PC_{61}BM$, electron acceptor) was a breakthrough in improvement of the efficiency [7]. Recently, tandem PSCs with a PCE of over 10% have been reported by J. You et al [8]. They used P3HT as a high band gap polymer for front cell and poly[2,7-(5,5-bis-(3,7-dimethyl octyl)-5H-dithieno[3,2-b:20,30-d]pyran)-alt-4,7-(5,6-difluoro-2,1,3-benzothiadiazole)] as a low band gap polymer for the rear cell. Thus, a tandem structure able to utilize the broader part of the solar spectrum is considered as the most effective method to increase PCE. In tandem structure, both high and low band gap polymers are necessary to absorb visible and near-infrared light in one device. Among

*Address correspondence to Y. S. Han, Department of Advanced Materials and Chemical Engineering, Catholic University of Daegu, 13-13 Hayang-ro, Hayang-eup, Gyeongsan-si, Gyeongbuk 712-702, Korea. E-mail: yshancu@cu.ac.kr

Color versions of one or more of the figures in the article can be found online at www.tandfonline.com/gmcl.

Downloaded by [East China University of Science and Technology] at 09:35 02 January 2016

various high band gap polymers, P3HT is one of the most-studied conjugated polymers due to its appropriate band gap energy (∼1.9 eV) for front cell, relatively high short circuit current density (J_{sc}) of over 10 mA/cm^2 and high external quantum efficiency of ∼70% [8–12].

The main limiting factors for high PCE in P3HT-based PSCs are poor exciton/charge transport and low absorption in the visible range of the solar spectrum in the active layer. The donor and acceptor materials should form nano-scaled interpenetrating networks within the whole active layer to ensure efficient exciton dissociation and charge transport [13]. Several interesting approaches to optimizating the morphology, such as thermal annealing at a specific temperature [14, 15], controlling the solvent evaporation rate [7], incorporating processing additives [16] or non-volatile additives into active layer [17], have been used to obtain nano-scaled bicontinuous phase in P3HT-based PSCs. Among these methods, the additive technique together with post thermal annealing is regarded as the best method to create nano-sized phase-separation in the active layer and molecular structural ordering within the nano-domains [18].

In a previous study [19], we reported on the effects of an additive, 4-cyano-4'-pentylbiphenyl (***5CB***), on the performance of PSCs. The addition of 3wt% ***5CB*** to a P3HT:PC_{61}BM blend film resulted in an improvement of over 22% compared to that of reference cell without ***5CB***. In this study, we further extended our simple additive technique to 4-cyano-4'-octylbiphenyl (***8CB***) to get a higher conversion efficiency of PSCs. PSCs with a configuration of ITO/PEDOT:PSS/P3HT:PC_{61}BM:***8CB***/LiF/Al were fabricated, and their photovoltaic properties were investigated.

Experimental Details

Materials

P3HT (98% regioregularity, $M_w = 6.4 \times 10^4$ g/mol) and PC_{61}BM were purchased from Rieke Metals and Nano-C, respectively. Poly-3,4-ethyleneoxythiophene:poly-4-sytrensulfonate (PEDOT:PSS, Baytron P VP Al 4083) was used as received from P. H. Stark GmbH. Solvents used in this study were all reagent grade and were used as received. ***8CB*** was purchased from Tokyo Chemical Industry Co., Ltd., and used without further purification. The chemical structure of the ***8CB*** additive in this study is shown in Figure 1.

Device Fabrication

PSCs were fabricated on indium-tin oxide (ITO) glasses (10 Ω/sq, SUNIC Ltd.) as follows. ITO glasses were cleaned by sequential ultrasonication in acetone, detergent, de-ionized water and isopropyl alcohol and then dried in a vacuum oven. Next, O_2 plasma treatment of the ITO glasses was conducted for 3 min, and immediately afterwards, PEDOT:PSS was spin-coated onto the ITO glass. The PEDOT:PSS films were then baked on a hot plate for 15 min at 140°C to yield a thickness of 30 nm; the film-coated ITO glass was then

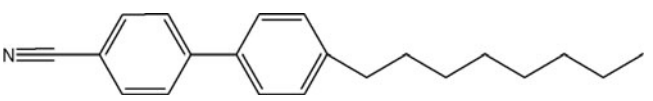

Figure 1. The chemical structure of ***8CB***.

Downloaded by [East China University of Science and Technology] at 09:35 02 January 2016

moved to a N_2 glove box for the remainder of the fabrication process. Regioregular P3HT and $PC_{61}BM$ at a weight ratio of 1:0.9 were first dissolved in chlorobenzene. Selected amounts of the ***8CB*** additive, ranging from 2 to 5 wt% based on the P3HT:$PC_{61}BM$, were then added to the P3HT:$PC_{61}BM$ solution, followed by stirring for 24 h at 50°C. The solution consisting of P3HT:$PC_{61}BM$ blended with additives was spin-cast onto the top of the PEDOT:PSS layer, and the plate was then dried on a hot plate in a covered Petri dish for 40 min at 50°C to produce an active layer with a thickness of 120 nm. Finally, a cathode consisting of LiF (1 nm) and a subsequent Al (100 nm) layer was deposited by thermal evaporation under a vacuum of 10^{-7} Torr. Devices with the configuration of ITO/PEDOT:PSS (30 nm)/P3HT:$PC_{61}BM$:***8CB*** (120 nm)/LiF (1 nm)/Al (100 nm) were encapsulated with a glass cap to protect them from air and then thermally annealed for 25 min at 145°C. The active area of all devices was determined to be 9 mm^2 using a shadow mask. Hole-only devices were fabricated with a diode configuration of ITO/PEDOT:PSS (30 nm)/P3HT:$PC_{61}BM$:***8CB*** (120 nm)/Pd (100 nm), where Pd with a high work function was used as an electrode to prevent the injection of electrons to LUMO (lowest unoccupied molecular orbital) energy level of $PC_{61}BM$. By replacing PEDOT:PSS with a Cs_2CO_3 layer spin-coated from its solution in 2-ethoxyethanol, electron-only devices were fabricated with a diode configuration of ITO/Cs_2CO_3/P3HT:$PC_{61}BM$:***8CB*** (120 nm)/LiF (1 nm)/Al (100 nm) for measuring electron mobility.

Characterization

UV-visible absorption spectra of the fabricated blend films with additive were obtained using a Perkin Elmer Lambda 750 UV/VIS spectrometer. The X-ray diffraction (XRD) profiles were measured using a BRUKER D8 ADVANCE with Cu Kα as the incident beam. Data were obtained from 3° to 50° (2θ) at a scan rate of 0.2 s/step. The atomic force microscopy (AFM) images were obtained in tapping mode on a Vecco multimode scanning probe microscope. Photocurrent-voltage measurements were performed with a Keithley model 2400 Source Meter and a Newport 91192 solar simulator system equipped with 1-kW xenon arc lamp from Oriel. The light intensity was adjusted to simulate AM 1.5 radiation at 100 mW cm^{-2} with a Radiant Power Energy Meter (model 70260, Oriel). Incident photon to current conversion efficiency (IPCE) results were acquired from an IPCE G1218a (PV measurement). All measurements were carried out under ambient conditions at room temperature.

Results and Discussion

The PSCs with configuration of ITO (150 nm)/PEDOT:PSS (30 nm)/P3HT:$PC_{61}BM$:***8CB*** (120 nm)/LiF (1 nm)/Al (100 nm) were fabricated and characterized after post-thermal annealing for 25 min at 145°C. To achieve the highest efficiency, the amount of ***8CB*** additive was varied from 2 to 5 wt%. The photovoltaic properties of the devices characterized under AM 1.5 conditions as a function of the amount of ***8CB*** are presented in Figure 2. In order to figure out the effects of ***8CB***, we here chose the PSC with the configuration of ITO (150 nm)/PEDOT:PSS (30 nm)/P3HT:$PC_{61}BM$ (120 nm)/LiF (1 nm)/Al (100 nm) as a reference device. The photovoltaic performance of the reference device without ***8CB*** was previously reported by us in this journal [19], i.e., a PCE of 3.56% with short circuit current (J_{sc}) = 19.24 mA/cm^2, open circuit voltage (V_{oc}) = 0.62V and fill factor (FF) = 55.98%. The PCEs of the devices with 2–5 wt% ***8CB*** were enhanced over that (3.56%) of the reference device (PSC0) without any additive. The annealed device (PSC4)

Downloaded by [East China University of Science and Technology] at 09:35 02 January 2016

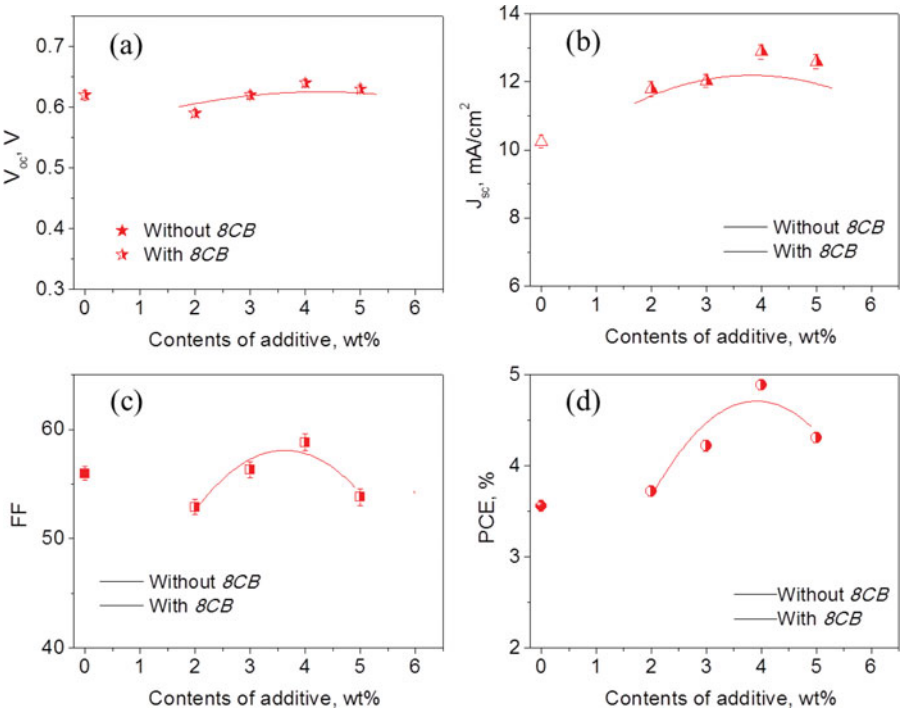

Figure 2. Performance variations with ***8CB*** concentration; (a) V_{oc}, (b) J_{sc}, (c) *FF* and (d) *PCE* of annealed PSCs under AM 1.5 irradiation.

with 4 wt% ***8CB*** exhibited the best performance due to an enhancement in J_{sc}, *FF* and V_{oc}, resulting in a PCE of 4.89% as compared to that (3.56%) of the control device (PSC0). Because the PCE exhibited the highest value when the ***8CB*** content was 4 wt%, we focused on this device with P3HT:$PC_{61}BM$:***8CB*** (4 wt%) blend film to determine the origin of the enhancement in efficiency. The photovoltaic properties of the annealed devices with and without ***8CB*** are summarized in Table 1, and the current density (*J*) versus voltage (*V*) curves are illustrated in Figure 3.

The enhanced PCE in the PSC with 4 wt% ***8CB*** was mainly due to an increase in J_{sc} (74% contribution). In PSCs, excitons created on conjugated polymers by light absorption are diffused to the interfaces between P3HT and $PC_{61}BM$, and then quickly separated into free electrons and holes. These charges are transported, through a combination of drift and diffusion, to their respective electrodes. Holes are transported by hopping between conjugated polymer segments, and electrons are transported by hopping between fullerene molecules. They are finally collected in electrodes. Thus, the J_{sc} value is related to exciton

Table 1. Photovoltaic properties of the reference device [19] and PSC with ***8CB***.

Annealed devices	Content of additive	V_{oc}, V	J_{sc}, mA/cm^2	*FF*,%	*PCE*,%
PSC0	0 wt%	0.62	10.25	55.98	3.56
PSC4	4 wt%	0.64	12.88	58.83	4.85

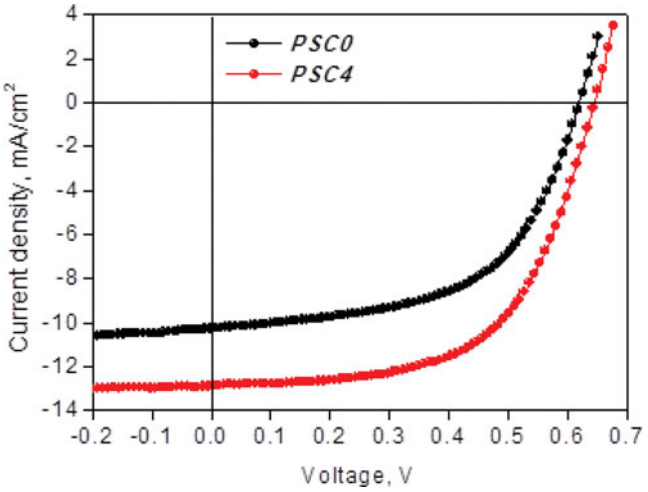

Figure 3. *J-V* characteristics of the reference device [19] and PSC with ***8CB***.

generation (η_{EG}), exciton diffusion (η_{ED}), charge separation (η_{CS}), charge transport (η_{CT}) and charge collection (η_{CC}) efficiency, and largely dependent on the η_{EG}, η_{ED}, and η_{CT}, since both the η_{CS} and η_{CC} are almost 100% [20]. The η_{EG} can be estimated from the absorption intensity, which is derived from the crystallinity of P3HT chains in photovoltaic blend films [14, 21]. In order to reveal the effects of η_{EG}, absorbance of the blend films were first measured. Figure 4 shows the UV-vis. absorption spectra of P3HT:PC_{61}BM blend films with and without 4 wt% ***8CB***, which were measured after thermal annealing at 145°C for 25 min with the same film thickness. Compared to the pristine P3HT:PC_{61}BM blend film, the film with ***8CB*** exhibited a higher absorbance in the major absorption peak (~520 nm) of the π-π^* transition and in the two vibronic peaks of 550 and 600 nm. These results clearly indicate that adding small amounts of ***8CB*** to the P3HT:PC_{61}BM blend film considerably

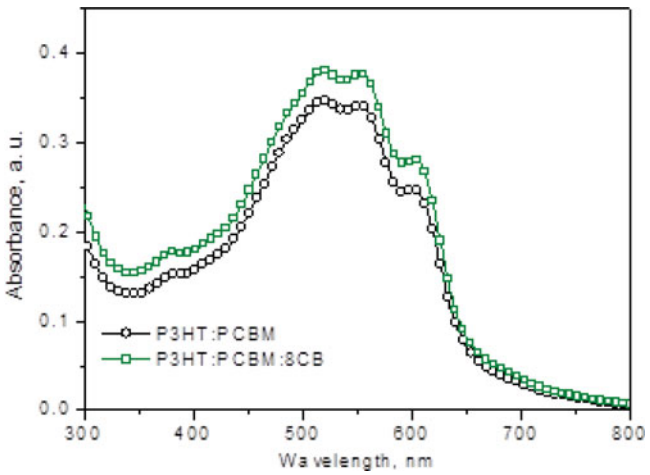

Figure 4. UV-vis absorption spectra of the P3HT:PC_{61}BM:***8CB*** and P3HT:PC_{61}BM [19] blend films.

Downloaded by [East China University of Science and Technology] at 09:35 02 January 2016

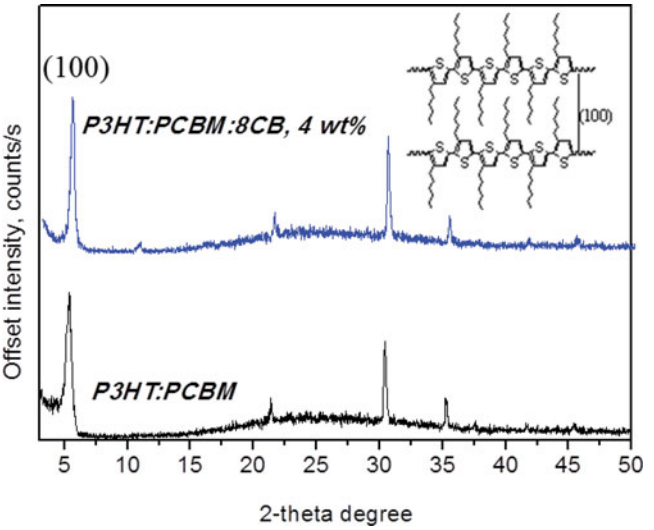

Figure 5. The X-ray diffractograms of the P3HT:$PC_{61}BM$:***8CB*** and P3HT:$PC_{61}BM$ [19] blend films. The peaks at $2\theta \approx 22^\circ$ and 31° arise from ITO [18,24], and the peak at $2\theta \approx 35^\circ$ is from $PC_{61}BM$ [25].

improved the crystallinity of P3HT chains, resulting in the enhancement in π-π^* transition efficiency of P3HT and thus an improvement in the η_{EG}.

The ordered structure and effective phase separation in P3HT:$PC_{61}BM$ blend films could increase the η_{CT}, because charge recombination could be reduced by them. The effect of ***8CB*** on the ordered structure of P3HT was investigated using X-ray diffraction (XRD) measurements. Figure 5 presents the XRD patterns of P3HT:$PC_{61}BM$ films with and without 4 wt% ***8CB*** on PEDOT:PSS/ITO glass. Intense $d_{(100)}$ peaks corresponding to an ordered lamellar structure with an interlayer spacing, which originated from interdigitated alkyl chains of P3HT, were observed in blend films. The diffraction peak intensity of the P3HT:$PC_{61}BM$:***8CB*** (5 wt%) film was increased over that of the pristine P3HT:$PC_{61}BM$ film, indicating that the crystallinity of P3HT was enhanced by the presence of ***8CB***. This result also suggests that ***8CB*** facilitates the phase separation of P3HT and $PC_{61}BM$, resulting in the high crystallinity of P3HT [22]. The average crystal size (L) of the P3HT in the P3HT:$PC_{61}BM$ films was calculated from the full width at half maximum (FWHM) of the $d_{(100)}$ peaks in the P3HT crystals using Scherrer's equation [23], $L = K\lambda / (B\ cos\theta)$, where λ is the incident X-ray wavelength, B is the FWHM of the diffraction $d_{(100)}$ peak, θ is the diffraction angle, and K is Scherrer's constant. The average crystal size of the P3HT in the P3HT:$PC_{61}BM$:***8CB*** (4 wt%) blend film was 21.16 nm, compared to that (15.96 nm) of the pristine P3HT:$PC_{61}BM$ film. The larger crystal size of P3HT could lead to more effective charge transport properties. We could also confirm the larger crystal size of P3HT by investigating the morphology of the active-layer films. The AFM images with a scan area of 5 μm $\times$ 5 μm were obtained from the blend films fabricated on top of the PEDOT:PSS-coated ITO glass. As can be seen in the tapping mode AFM images in Figure 6, the grain size processed with ***8CB*** was much bigger than that without an additive. This result is further evidence of the effective phase separation of P3HT and $PC_{61}BM$ with the aid of additives. Thus, higher crystallinty and larger crystal size in the P3HT:$PC_{61}BM$:***8CB*** blend film can lead to more effective phase separation, yielding an enhancement in the η_{CT}.

Downloaded by [East China University of Science and Technology] at 09:35 02 January 2016

Downloaded by [East China University of Science and Technology] at 09:35 02 January 2016

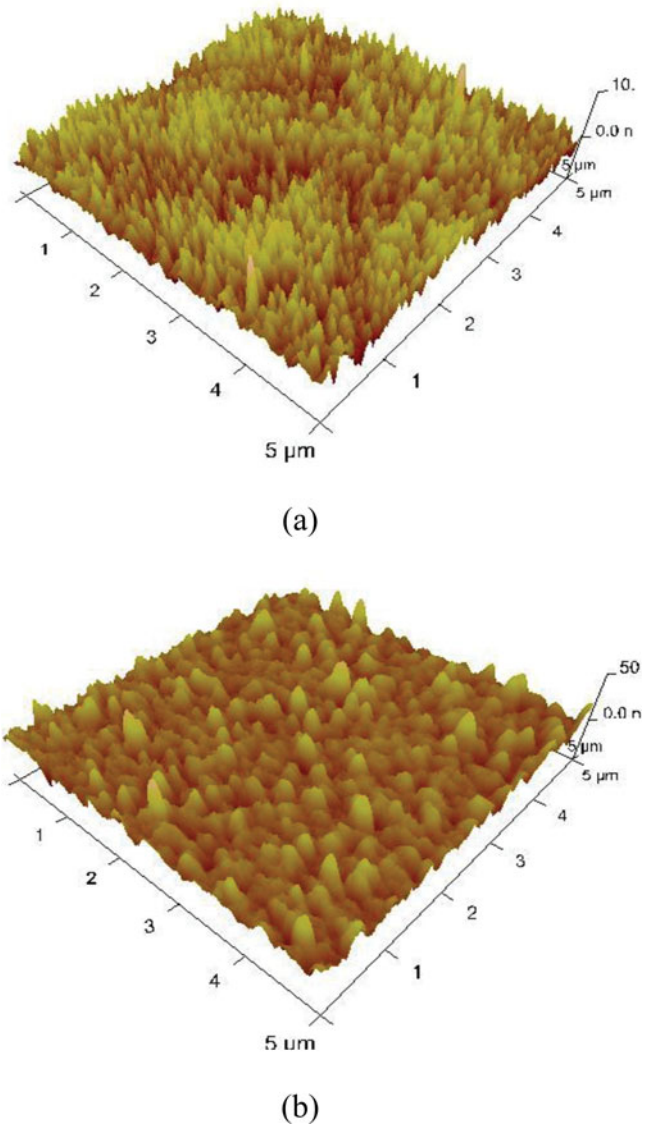

Figure 6. AFM 3D images of the P3HT:$PC_{61}BM$ and P3HT:$PC_{61}BM$:***8CB*** surfaces.

The smaller value of mean interlayer spacing of P3HT also plays an important role in increasing charge transport in the active layer. Using Bragg's equation $n\lambda = 2d\sin\theta$ [26], where n, λ, d and θ denote the order of diffraction, the wavelength of an X-ray beam, the interlayer spacing, and the Bragg angle, respectively, the mean interlayer spacing of the P3HT in the films with 8CB was calculated as 16.5 Å, compared to that (16.6 Å) of the film without 8CB. This result implies that the interaction between P3HT is stronger with the presence of 8CB, resulting in better packed P3HT chains. Closer packing of P3HT chains can contribute to an enhancement in J_{sc} due to a lower resistance to the hopping of carriers between P3HT backbones. This is another piece of evidence for the enhancement in the η_{CT}.

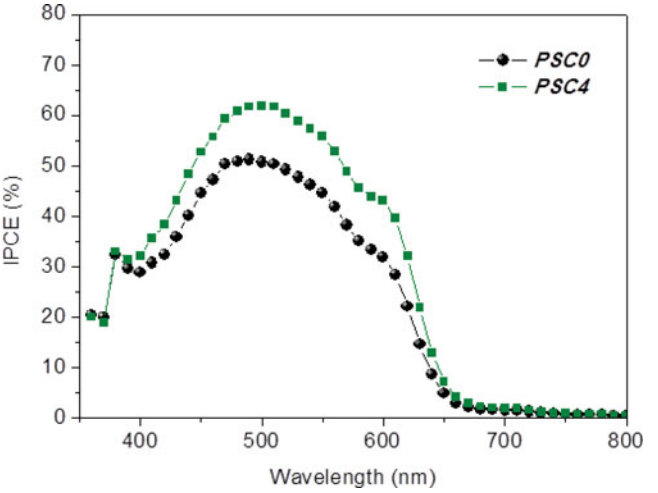

Figure 7. IPCE spectra of the annealed PSCs with and without ***8CB***.

The results obtained from absorption spectroscopy, X-ray measurements and AFM images clearly indicate that the ***8CB*** in the P3HT:$PC_{61}BM$ film enhances the ordering (crystallization) of the P3HT and phase separation, resulting in an improvement in both η_{EG} and η_{CT}, and thus the increment in J_{sc}. The increased J_{sc} is furthermore supplemented through the results of improved IPCE. The IPCE spectra of the annealed devices are compared in Figure 7. The two IPCE curves display results consistent with the trend in J_{sc}. The enhanced IPCEs across a broad spectral range could be attributed to the improved crystallization of the closer packing of P3HT by a small amount of additive**.**

The *FF* value of the PSC with the P3HT:$PC_{61}BM$:***8CB*** blend film was also increased (16% contribution) compared to the reference device as shown in Table 1. It is generally accepted that the *FF* is influenced by the balance between hole and electron mobilities in PSCs because it is limited by the carrier drift length, which is defined as (carrier mobility) x (carrier recombination lifetime) x (electric field) [18, 27]. Space charge limited current (SCLC) measurements have been used to evaluate charge mobility under steady state currents in organic layers [28, 29]. According to SCLC criteria, a half-power dependence of the photocurrent on the applied voltage is observed, and the *FF* cannot be above 40%. However, when the carrier transport is more balanced, the current is not limited by space-charge effects, and high *FF*s are possible [7].

Using the SCLC method, the hole mobility of the devices was studied to confirm the effect of the additive on the *FF* of the annealed devices. The current density in the SCLC model is given by equation (1).

$$J = \frac{9}{8}\varepsilon_r \varepsilon_0 \mu_{h0} \frac{V^2}{L^3} \exp\left(0.89\sqrt{\frac{V}{E_0 L}}\right) \tag{1}$$

Here, ε_r is the dielectric constant of the polymer (assumed to be 3, which is a typical value for conjugated polymers) [30, 31], ε_0 is the permittivity of free space, μ_{h0} (or μ_{e0}) is the zero-field hole (or electron) mobility, L is the film thickness, and E_0 is the characteristic field. $V = V_{appl} - (V_r + V_{bi})$, where V_{appl} is the voltage applied to the device, V_r is the voltage drop due to series resistance across the electrodes and V_{bi} is the built-in voltage. The hole

Downloaded by [East China University of Science and Technology] at 09:35 02 January 2016

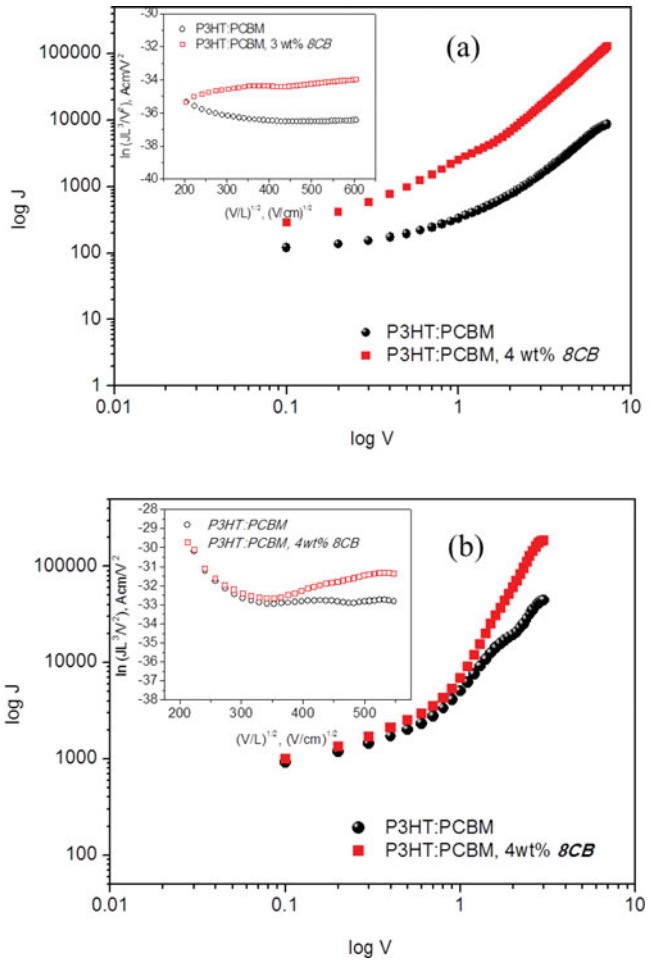

Figure 8. J-V characteristics of the hole-only (a) and electron-only (b) devices with and without [19] ***8CB*** measured in the dark.

mobilities of the devices were calculated from equation (1) using the *J-V* curves of the hole-only devices [28] with the configuration of ITO/PEDOT:PSS(30 nm)/P3HT:$PC_{61}BM$:with or without ***8CB*** (120 nm)/Pd(100 nm), which can obstruct the electron injection from the cathode due to the large mismatch between the LUMO energy level (4.30 eV) of $PC_{61}BM$ [11] and the work function (5.12 eV) of the Pd electrode [32]. The experimental dark current densities of the annealed hole-only devices with or without ***8CB*** are shown in Figure 8(a). The results are also plotted as the logarithm of JL^3/V^2 versus the square root of *V/L*, as shown in the inset of Figure 8(a). In the inset graph, the intercept of this line represents the hole mobility. The hole mobility of the device with 4 wt% ***8CB*** increased from 2.8×10^{-5} [19] to 1.3×10^{-4} $cm^2/V{\cdot}s$, one order of magnitude higher than that of the device without ***8CB***. This result was well consistent with the larger crystal size and closer packing of P3HT chains, described earlier.

Meanwhile, electron-only devices with the configurations ITO/Cs_2CO_3/P3HT:$PC_{61}BM$:with or without ***8CB***/LiF/Al, in which Cs_2CO_3 layer [29] transports

Downloaded by [East China University of Science and Technology] at 09:35 02 January 2016

electrons from LUMO energy level of $PC_{61}BM$ to ITO and blocks holes from ITO to HOMO (highest occupied molecular orbital) energy level of P3HT were fabricated, and then the electron mobilities of the electron-only devices were calculated using equation (1) and measured J-V data [Figure 8(b)]. The electron mobility changed very little from 5.0 $\times$ 10^{-3} [19] for the control device to 7.1 $\times$ 10^{-3} $cm^2/V{\cdot}s$ for the device with ***8CB***. Based on the calculated hole and electron mobilities, the ratio (μ_e/μ_h) of the hole and electron mobility for the devices with ***8CB*** was determined to be 55 as compared to that (178) of the device without ***8CB*** [19].

Due to an enhanced and balanced charge transport in the device with the ***8CB*** additive, a higher *FF* was achieved [33]. The photovoltaic performance of devices with a thicker active layer than the mean carrier drift length of the charge carrier is limited by the carrier with a lower mean free path (holes in PSCs) [34]. To maintain the electrical neutrality in the device, the unbalanced transport will result in loss of efficiency due to increased charge recombination. Significant enhancement of hole mobility by the addition of ***8CB*** into the active layer yields more balanced transport of holes and electrons, and hence reduces the accumulation of space charges in films and hole-electron recombination loss, leading to an enhancement of the *FF* [35, 36].

The V_{oc} value was slightly enhanced from 0.62 to 0.64 V, corresponding to 10% contribution to the improvement in PCE (Table 1). Because the V_{oc} is linearly related to the $HOMO_{donor}$-$LUMO_{acceptor}$ energy difference [37], which is directly correlated with acceptor strength, the relatively small increase in V_{oc} indicates that the acceptor strength in PSCs was slightly changed by the presence of ***8CB*** in the P3HT:$PC_{61}BM$ blend film.

Conclusion

In summary, we have demonstrated effects of ***8CB*** as an additive on the performance of PSC based on P3HT:$PC_{61}BM$ blend film by monitoring UV-visible absorption spectra, X-ray diffractograms, AFM images and carrier mobilities. The PSC with P3HT:PCBM:8CB blend film showed the J_{sc} of 12.88 mA/cm^2, the V_{oc} of 0.64V and the *FF* of 58.83%, compared to the J_{sc} of 10.25 mA/cm^2, the V_{oc} of 0.62V and the *FF* of 55.98% for the reference device P3HT:PCBM blend film (without 8CB). The improved PCE of PSC with three-component active layer was attributed to a higher absorbance, larger crystal size, closer packing of P3HT, and hence enhanced hole mobility. Thus, by the choice of useful additive, we could get a higher PCE in the PSC.

Acknowledgment

This work was supported by research grants from the Catholic University of Daegu in 2014.

References

[1] Yu, G., Gao, j., Hummelen, J. C., Wudl, F., & Heeger, A. J. (1995). *Science*, *270*, 1789.
[2] Brabec, C. J., Sariciftci, N. S., & Hummelen, J. C. (2001). *Adv. Funct. Mater. 11*, 15.
[3] Gunes, S., Neugebauer, H., & Sariciftci, N. S. (2007). *Chem. Rev.*, *107*, 1324.
[4] Li, G., Zhu, R., & Yang, Y. (2012). *Nat. Photonics 6*, 153.
[5] Hadipour, A., de Boer, B., & Blom, P. W. M. (2008). *Adv. Funct. Mater. 18*, 169.
[6] Cai, W., Gong, X., & Cao, Y. (2010). *Sol. Energy Mater. Sol. Cells 94*, 114.
[7] Li, G., Shrotriya, V., Huang, J., Yao, Y., Moriarty, T., Emery, K., & Yang, Y. (2005). *Nat. Mater.*, *4*, 864.

Downloaded by [East China University of Science and Technology] at 09:35 02 January 2016

[8] You, J., Dou, L., Yoshimura, K., Kato, T., Ohya, K., Moriarty, T., Emery, K., Chen, C.-C., Gao, J., Li, G., & Yang, Y. (2013). *Nat. Commun.*, *4*, 1446.
[9] Fan, X., Guo, S., Fang, G., Zhan, C., Wang, H., Zhang, Z., & Li, Y. (2013). *Sol. Energy Mater. Sol. Cells*, *113*, 135.
[10] Dou, L., You, J., Yang, J., Chen, C.-C., He, Y., Murase, S., Moriarty, T., Emery, K., Li, G., & Yang, Y. (2012). *Nat. Photonics*, *6*, 180.
[11] Kim, J. Y., Lee, K., Coates, N. E., Moses, D., Nguyen, T.-Q., Dante, M., & Heeger, A. J. (2007). *Science*, *317*, 222.
[12] Zhou, Y., Fuentes-Hernandez, C., Shim, J. W., Khan, T. M., & Kippelen, B. (2012). *Energy Environ. Sci.*, *5*, 9827.
[13] Sivula, K., Ball, Z. T., Watanabe, N. & Fréchet, J. M. M. (2006). *Adv. Mater. 18*, 206.
[14] Nguyen, L. H., Hoppe, H., Erb, T., Günes, S., Gobsch, G. & Sariciftci, N. S. (2007). *Adv. Funct. Mater. 17*, 1071.
[15] Kim, K, Liu, J., Namboothiry, M. A. G., & Carroll, D. L. (2007). *Appl. Phys. Lett.*, *90*, 163511.
[16] Peet, J. Senatore, M. L., Heeger, A. J., & Bazan, G. C. (2009). *Adv. Mater. 21*, 1521.
[17] Kim, C. S., Tinker, L. L., DiSalle, B. F., Gomez, E. D., Lee, S., Bernhard, S. & Loo, Y.-L. (2009). *Adv. Mater. 21*, 3110.
[18] Ma, W., Yang, C., Gong, X., Lee, K., & Heeger, A. J. (2005). *Adv. Funct. Mater. 15*, 1617.
[19] Han, Y. S. (2013). *Mol. Cryst. Liq. Cryst. 586*, 43.
[20] Peumans, P. & Forrest, S. R. (2004), *Chem. Phys. Lett. 398*, 27.
[21] Zhao, Y., Xie, Z., Qu, Y., Geng, Y., & Wang, L. (2007). *Appl. Phys. Lett. 90*, 043504.
[22] Chen, H.–Y., Yang, H., Yang, G., Sista, S., Zadoyan, R., Li, G., & Yang, Y. (2009). *J. Phys. Chem. C113*, 7946.
[23] Briks, L. S., & Friedman, H. (1946). *J. Appl. Phys.*, *17*, 687.
[24] Erb, T., Zhokhavets, U., Gobsch, G., Raleva, S., Stuhn, B., Schilinsky, P., Waldauf, C., & Brabec, C. J. (2005). *Adv. Funct. Mater.*, *15*, 1193.
[25] Reyes-Reyes, M., López-Sandoval, R., Arenas-Alatorre, J., Garibay-Alonso, R., Carroll, D. L., & Lastras-Martinez, A. (2007). *Thin Solid Films*, *516*, 52.
[26] Chiu, M.-Y., Jeng, U. S., Su, C.-H., Liang, K. S., & Wei, K.-H. (2008). *Adv. Mater 20*, 2573.
[27] Koster, L. J. A., Mihailetchi, V. D., & Blom, P. W. M. (2006). *Appl. Phys. Lett.*, *88*, 093511.
[28] Chirvase, D., Chiguvare, Z., Knipper, M., Paris, J., Dyakonov, V., & Hummelen, J. C. (2003). *J. Appl. Phys.*, *93*, 3376.
[29] Shrotriya, V., Yao, Y., Li, G., & Yang, Y. (2006). *Appl. Phys. Lett.*, *89*, 063505.
[30] Kim S.-O., Chung, D. S., Cha, H., Jang, J. W., Kim, Y.-H., Kang, J.-W., Jeong, Y.-S., Park, C. E., & Kwon, S.-K. (2011). *Sol. Energy Mater. Sol. Cells*, *95*, 432.
[31] Zhou, H., Yang, L., Stoneking, S., & You, W. (2010). *ACS Appl Mater Interfaces*, *2*, 1377.
[32] Gu, D., Deya, S. K., & Majhi, P. (2006). *Appl. Phys. Lett.*, *89*, 082907.
[33] Chiu, M., Jeng, U., Su, M., & Wei, K. (2010). *Macromolecules*, *43*, 428.
[34] Snaith, H. L., Greenham, N. C., & Friend, R. H. (2004). *Adv. Mater.*, *16*, 1640.
[35] Shin, C. F., Hung, K. T., Wu, J. W., Hsiao, C. Y., & Li, W. M. (2009). *Appl. Phys. Lett.*, *94*, 143505.
[36] Liu, J., Shao, S., Wang, H., Zhao, K., Xue, L., Gao, X., Xie, Z., & Han, Y. (2010). *Org. Electron.*, *11*, 775.
[37] Scharber, M. C., Műhlbacher, D., Koppe, M., Denk, P., Waldauf, C., Heeger, A. J., & Brabec, C. J. (2006). *Adv. Mater.*, *18*, 789.

Downloaded by [East China University of Science and Technology] at 09:35 02 January 2016